

Rayleigh scattering of twisted light by hydrogenlike ions

A. A. Peshkov,^{1,*} A. V. Volotka,^{1,2} A. Surzhykov,^{3,4} and S. Fritzsche^{1,5}

¹*Helmholtz-Institut Jena, D-07743 Jena, Germany*

²*Department of Physics, St. Petersburg State University, 198504 St. Petersburg, Russia*

³*Physikalisch-Technische Bundesanstalt, D-38116 Braunschweig, Germany*

⁴*Technische Universität Braunschweig, D-38106 Braunschweig, Germany*

⁵*Theoretisch-Physikalisches Institut & Abbe Center of Photonics,*

Friedrich-Schiller-Universität Jena, D-07743 Jena, Germany

(Dated: March 2, 2022)

The elastic Rayleigh scattering of twisted light and, in particular, the polarization (transfer) of the scattered photons have been analyzed within the framework of second-order perturbation theory and Dirac's relativistic equation. Special attention was paid hereby to the scattering on three different atomic targets: single atoms, a mesoscopic (small) target, and a macroscopic (large) target, which are all centered with regard to the beam axis. Detailed calculations of the polarization Stokes parameters were performed for C^{5+} ions and for twisted Bessel beams. It is shown that the polarization of scattered photons is sensitive to the size of an atomic target and to the helicity, the opening angle, and the projection of the total angular momentum of the incident Bessel beam. These computations indicate more that the Stokes parameters of the (Rayleigh) scattered twisted light may significantly differ from their behaviour for an incident plane-wave radiation.

PACS numbers: 31.10.+z, 32.80.Wr, 42.50.Tx

Keywords: elastic scattering, atoms, Dirac equation, transitions, polarization, optical vortex, OAM

I. INTRODUCTION

The elastic scattering of photons at the bound electrons of atoms or ions, commonly known as Rayleigh scattering, has been intensively explored over the past decades [1–3]. From a theoretical viewpoint, the Rayleigh scattering has attracted much interest as one of the simplest second-order quantum electrodynamical (QED) process [4]. From a practical viewpoint, detailed knowledge of the properties of elastically scattered photons has been found important for applications in material research [5], medical imaging [6], and astrophysics [7].

In the past, a large number of experimental and theoretical studies have been performed in order to understand how the electronic structure of atoms affects the polarization of the Rayleigh-scattered photons [8–16]. In particular, the linear polarization of the elastically scattered light has been measured directly by Blumenhagen *et al.* at the PETRA III synchrotron at DESY [17]. This experiment was performed for a gold target with a highly linearly polarized incident plane-wave radiation. Until the present, however, very little is known about the Rayleigh scattering of twisted (or vortex) light beams. When compared to plane-wave radiation, such twisted photons have a helical wavefront and carry a well-defined projection of the orbital angular momentum (OAM) upon their propagation direction [18, 19]. In addition, the transverse intensity profile of the twisted beams exhibits a ringlike pattern with a dark spot (vortex) at the center [20]. In experiments, twisted (Bessel) beams can nowadays be readily produced by means of

spatial light modulators [21] or axicons [22–24]. During recent years a number of studies have shown that the OAM and the intensity profile of these twisted beams may affect different fundamental light-matter interaction processes such as the Compton scattering [25–27], photoexcitation [28–33] and photoionization [34, 35] of atoms, the generation of electric currents in quantum rings [36] and molecules [37], electromagnetically induced transparency [38], four-wave mixing in atomic vapors [39]. One might therefore expect that the “twistedness” of incoming radiation will affect also the polarization of outgoing photons in the Rayleigh scattering.

In the present work, we analyze theoretically the behavior of the polarization Stokes parameters of scattered photons for the elastic scattering of twisted Bessel light. Here we restrict ourselves to the nonresonant Rayleigh scattering of light by hydrogenlike ions in their ground state, and especially by C^{5+} ions. In Sec. II, we shall consider and derive the Stokes parameters within the framework of second-order perturbation theory and the density matrix approach. Three different “experimental” scenarios are considered here for the scattering of the incident Bessel beam at: (i) a single atom, (ii) a mesoscopic (small) or (iii) a macroscopic (large) atomic target, and which are all assumed to be centered on the beam axis. Results of our calculations for the Bessel beams with different polarizations, opening angles, and projections of the total angular momentum (TAM) are presented in Sec. III and are compared with those for incident plane-wave radiation. These results demonstrate that the scattering of twisted light may lead to well detectable changes in the polarization of scattered photons. Finally, a summary and outlook are given in Sec. IV.

Atomic units ($\hbar = 4\pi\epsilon_0 = e = m_e = 1, c = 1/\alpha$) are

* anton.peshkov@uni-jena.de

used throughout the paper unless stated otherwise.

II. THEORY

A. Vector potential of Bessel light beams

Before we consider the Rayleigh scattering of twisted Bessel beams on atoms, let us first define and explain such beams of light. In general, all the properties of light can be described by means of the vector potential. For a Bessel beam with a well-defined helicity λ_1 , longitudinal momentum k_{z_1} , (modulus of the) transverse momentum \varkappa , photon energy $\omega = ck_1 = c\sqrt{k_{z_1}^2 + \varkappa^2}$, as well as the projection m of the total angular momentum (TAM) upon its propagation (z) direction, for instance, the vector potential is given by [35]

$$\mathbf{A}^{\text{tw}}(\mathbf{r}) = \int a_{\varkappa m}(\mathbf{k}_{\perp 1}) \mathbf{e}_{\mathbf{k}_1 \lambda_1} e^{i\mathbf{k}_1 \mathbf{r}} \frac{d^2 \mathbf{k}_{\perp 1}}{(2\pi)^2}, \quad (1)$$

where the amplitude $a_{\varkappa m}(\mathbf{k}_{\perp 1})$ is of the form

$$a_{\varkappa m}(\mathbf{k}_{\perp 1}) = (-i)^m e^{im\phi_{k_1}} \sqrt{\frac{2\pi}{k_{\perp 1}}} \delta(k_{\perp 1} - \varkappa). \quad (2)$$

As seen from these expressions, such a Bessel beam can be considered also as a superposition of circularly polarized plane waves $\mathbf{e}_{\mathbf{k}_1 \lambda_1} e^{i\mathbf{k}_1 \mathbf{r}}$ with well-defined helicity λ_1 . Their wave vectors \mathbf{k}_1 are uniformly distributed upon the surface of a cone with an opening angle $\theta_{k_1} = \arctan(\varkappa/k_{z_1})$ and are orthogonal to the polarization vectors, $\mathbf{e}_{\mathbf{k}_1 \lambda_1} \cdot \mathbf{k}_1 = 0$.

Although the integral representation (1) of the vector potential $\mathbf{A}^{\text{tw}}(\mathbf{r})$ is very convenient for atomic calculations, it is useful to perform the integration over $\mathbf{k}_{\perp 1}$ in Eq. (1) explicitly, in particular for very small opening angles θ_{k_1} for which the transverse momentum is much smaller than the longitudinal one, $\varkappa \ll k_{z_1}$. Within this (so-called) paraxial approximation, this integration gives then rise to a vector potential (up to a multiplicative constant) in the form [34]

$$\mathbf{A}^{\text{tw}}(\mathbf{r}) = \varepsilon_{\lambda_1} J_{m-\lambda_1}(\varkappa r_{\perp}) e^{i(m-\lambda_1)\phi} e^{ik_{z_1}z}, \quad (3)$$

and where $J_{m-\lambda_1}(\varkappa r_{\perp})$ denotes the Bessel function of the first kind. Substituting the polarization vector $\varepsilon_{\lambda_1} = \mathbf{e}_{\mathbf{k}_1 \lambda_1} (\theta_{k_1} = \phi_{k_1} = 0^\circ)$ into this expression, we see that the Bessel beam with a small opening angle has well-defined projections of the orbital $m-\lambda_1$ (OAM) and spin λ_1 (SAM) angular momenta onto the z axis. However, such a decoupling of the OAM and SAM does not longer apply in the nonparaxial regime, i.e., when the opening angle θ_{k_1} becomes larger [34].

B. Evaluation of the transition amplitude

With this brief account on the vector potential of twisted Bessel beams, we can now discuss the Rayleigh scattering of such beams by hydrogenlike ions. We here begin from the Furry picture of QED, in which the electron-nucleus interaction is included into the unperturbed Hamiltonian, while the interaction with the radiation field is treated as a perturbation [4]. In this picture, the properties of the scattered photons can all be obtained from the second-order transition amplitude, based on Dirac's relativistic equation. In this framework, the amplitude is given by [13, 40]

$$\begin{aligned} \mathcal{M}_{m_f m_i}^{\lambda_2 \lambda_1}(\mathbf{b}) &= \sum_{n_\nu j_\nu m_\nu} \frac{\langle n_f j_f m_f | \boldsymbol{\alpha} \cdot \mathbf{A}^{\text{Pl}*}(\mathbf{r}) | n_\nu j_\nu m_\nu \rangle \langle n_\nu j_\nu m_\nu | \boldsymbol{\alpha} \cdot \mathbf{A}^{\text{tw}}(\mathbf{r} + \mathbf{b}) | n_i j_i m_i \rangle}{E_i - E_\nu + \omega} \\ &+ \sum_{n_\nu j_\nu m_\nu} \frac{\langle n_f j_f m_f | \boldsymbol{\alpha} \cdot \mathbf{A}^{\text{tw}}(\mathbf{r} + \mathbf{b}) | n_\nu j_\nu m_\nu \rangle \langle n_\nu j_\nu m_\nu | \boldsymbol{\alpha} \cdot \mathbf{A}^{\text{Pl}*}(\mathbf{r}) | n_i j_i m_i \rangle}{E_i - E_\nu - \omega}, \end{aligned} \quad (4)$$

where $|n_i j_i m_i\rangle$ and $|n_f j_f m_f\rangle$ denote the states of the hydrogenlike ion before and after the scattering, and where $j_{i,f}$ and $m_{i,f}$ refer to the total angular momenta and their projections, and $n_{i,f}$ stand for principal quantum numbers. We here restrict ourselves to the nonresonant elastic scattering of the photons with the energy ω on the ground state of atoms. This implies that the total energy of the bound electron for the initial and final states of the atom with $n_i = n_f$ and $j_i = j_f$ obeys the energy conservation law $E_i = E_f$, and that the photon energy ω

is not close to possible excitations of any intermediate states $|n_\nu j_\nu m_\nu\rangle$ over which the summation in the matrix element (4) is carried out, i.e., $\omega \neq E_\nu - E_i$.

In the matrix element (4), the interaction of the atomic electrons with an incident Bessel beam is described by the transition operator $\boldsymbol{\alpha} \cdot \mathbf{A}^{\text{tw}}(\mathbf{r} + \mathbf{b})$, where $\boldsymbol{\alpha}$ denotes the vector of the Dirac matrices and \mathbf{A}^{tw} is the vector potential of the beam as given by Eq. (1). Here, the impact parameter \mathbf{b} occurs because the electron (coordinates) is shifted with regard to the beam axis. Since equation

(3) implies that the Bessel beam exhibits an inhomogeneous intensity distribution and a ringlike pattern in the transverse plane (cf. Fig. 1), the Rayleigh scattering will explicitly depend on the atomic impact parameter $\mathbf{b} = (b_x, b_y, 0)$.

In Eq. (4), we assumed that the scattered photons are plane waves $\mathbf{A}^{p1}(\mathbf{r}) = \mathbf{e}_{\mathbf{k}_2\lambda_2} e^{i\mathbf{k}_2\mathbf{r}}$ with $k_2 = k_1 = \omega/c$ measured by a detector placed at asymptotic distance under the direction \mathbf{k}_2 . This is a reasonable assumption since all presently available detectors are plane wave detectors. To further analyze the transition amplitude (4), we can decompose the plane-wave components of the incident and outgoing radiation in terms of the electric and magnetic multipole fields. When the wave vectors

$\hat{\mathbf{k}}_1 = (\theta_{k_1}, \phi_{k_1})$ and $\hat{\mathbf{k}}_2 = (\theta_{k_2}, \phi_{k_2})$ are not both directed along the quantization z axis, this decomposition may be written as

$$\mathbf{e}_{\mathbf{k}\lambda} e^{i\mathbf{k}\mathbf{r}} = \sqrt{2\pi} \sum_{LM} \sum_{p=0,1} i^L \sqrt{2L+1} \times (i\lambda)^p D_{M\lambda}^L(\phi_k, \theta_k, 0) \mathbf{a}_{LM}^p(\mathbf{r}). \quad (5)$$

Here $D_{M\lambda}^L$ is the Wigner D function, and $\mathbf{a}_{LM}^p(\mathbf{r})$ refers to the magnetic ($p = 0$) and electric ($p = 1$) multipole components, respectively [41]. If we substitute the multipole expansion (5) into Eq. (4) and make use of the vector potential (1) of Bessel beams, we can rewrite the transition amplitude as

$$\mathcal{M}_{m_f m_i}^{\lambda_2 \lambda_1}(\mathbf{b}) = \sum_{M_1} \int a_{\mathcal{Z}m}(\mathbf{k}_{\perp 1}) e^{-iM_1 \phi_{k_1} + i\mathbf{k}_{\perp 1} \mathbf{b}} T_{m_f m_i}^{\lambda_2 \lambda_1}(M_1) \frac{d^2 \mathbf{k}_{\perp 1}}{(2\pi)^2} \quad (6)$$

with the function $T_{m_f m_i}^{\lambda_2 \lambda_1}(M_1)$ of the form

$$\begin{aligned} T_{m_f m_i}^{\lambda_2 \lambda_1}(M_1) = & \sum_{L_1 p_1} \sum_{L_2 M_2 p_2} 2\pi i^{L_1 - L_2} \sqrt{(2L_1 + 1)(2L_2 + 1)} (i\lambda_1)^{p_1} (-i\lambda_2)^{p_2} e^{iM_2 \phi_{k_2}} d_{M_1 \lambda_1}^{L_1}(\theta_{k_1}) d_{M_2 \lambda_2}^{L_2}(\theta_{k_2}) \\ & \times \sum_{j_\nu} \left(\frac{\langle j_i m_i, L_1 M_1 | j_\nu m_\nu \rangle \langle j_\nu m_\nu, L_2 M_2 | j_f m_f \rangle}{\sqrt{(2j_\nu + 1)(2j_f + 1)}} S_{L_2 p_2, L_1 p_1}^{j_\nu}(\omega) \right. \\ & \left. + \frac{\langle j_i m_i, L_2 M_2 | j_\nu m_\nu \rangle \langle j_\nu m_\nu, L_1 M_1 | j_f m_f \rangle}{\sqrt{(2j_\nu + 1)(2j_f + 1)}} S_{L_1 p_1, L_2 p_2}^{j_\nu}(-\omega) \right), \quad (7) \end{aligned}$$

where we have used the Wigner small d function and the Wigner-Eckart theorem [42]. The reduced second-order matrix element is given by

$$S_{L_1 p_1, L_2 p_2}^{j_\nu}(\pm\omega) = \sum_{n_\nu} \frac{\langle n_f j_f | \boldsymbol{\alpha} \cdot \mathbf{a}_{L_1}^{p_1} | n_\nu j_\nu \rangle \langle n_\nu j_\nu | \boldsymbol{\alpha} \cdot \mathbf{a}_{L_2}^{p_2} | n_i j_i \rangle}{E_i - E_\nu \pm \omega}. \quad (8)$$

To further simplify the matrix element (6), we perform the integration over $k_{\perp 1}$ and ϕ_{k_1} with the help of Eq. (2) and by making use of the integral representation of the Bessel function [33]

$$\begin{aligned} & \frac{1}{2\pi} \int_0^{2\pi} e^{i(m-M_1)\phi_{k_1} + i\mathcal{Z}b \cos(\phi_{k_1} - \phi_b)} d\phi_{k_1} \\ & = i^{m-M_1} e^{i(m-M_1)\phi_b} J_{m-M_1}(\mathcal{Z}b). \quad (9) \end{aligned}$$

With this substitution, the transition amplitude for the scattering on a single hydrogenlike ion can be written as

$$\begin{aligned} \mathcal{M}_{m_f m_i}^{\lambda_2 \lambda_1}(\mathbf{b}) = & \sqrt{\frac{\mathcal{Z}}{2\pi}} \sum_{M_1} (-i)^{M_1} e^{i(m-M_1)\phi_b} \\ & \times J_{m-M_1}(\mathcal{Z}b) T_{m_f m_i}^{\lambda_2 \lambda_1}(M_1). \quad (10) \end{aligned}$$

As seen from this formula, the amplitude for the scattering of a Bessel beam depends not only on its helicity

λ_1 , the opening angle θ_{k_1} and the projection m of the TAM, but also on the impact parameter \mathbf{b} of the atom with respect to the beam axis. Below, we shall apply this transition amplitude to calculate the polarization of scattered light.

C. Scattering on a single atom

To characterize the polarization of scattered photons, we need to introduce the photon density matrix. For the scattering of twisted light on a single initially unpolarized atom with the impact parameter \mathbf{b} , the density matrix of scattered photons can be expressed in terms of the

transition amplitudes as [43]

$$\begin{aligned} \langle \mathbf{k}_2 \lambda_2 | \hat{\rho}_{\gamma_2} | \mathbf{k}_2 \lambda_2' \rangle &= \frac{1}{2j_i + 1} \sum_{\lambda_1 \lambda_1'} \sum_{m_i m_f} \mathcal{M}_{m_f m_i}^{\lambda_2 \lambda_1}(\mathbf{b}) \\ &\times \mathcal{M}_{m_f m_i}^{\lambda_2' \lambda_1'}(\mathbf{b}) \langle \mathbf{k}_1 \lambda_1 | \hat{\rho}_{\gamma_1} | \mathbf{k}_1 \lambda_1' \rangle. \end{aligned} \quad (11)$$

Here we assume that the magnetic sublevel population of the final state $|n_f j_f\rangle$ of the atom remains unob-

served. The density matrix of an incident photon is $\langle \mathbf{k}_1 \lambda_1 | \hat{\rho}_{\gamma_1} | \mathbf{k}_1 \lambda_1' \rangle = \delta_{\lambda_1 \lambda_1'}$ for a completely polarized radiation with the helicity λ_1 . In typical experiments, however, the incident light is often unpolarized, i.e., the beam consists out of a mixture of photons in states of opposite helicity $\lambda_1 = \pm 1$ with equal intensities whose density matrix is $\langle \mathbf{k}_1 \lambda_1 | \hat{\rho}_{\gamma_1} | \mathbf{k}_1 \lambda_1' \rangle = 1/2 \delta_{\lambda_1 \lambda_1'} \delta_{\lambda_1 + 1} + 1/2 \delta_{\lambda_1 \lambda_1'} \delta_{\lambda_1 - 1}$. Using the explicit expression of the amplitude (10), we can rewrite the density matrix of scattered photons in the form

$$\begin{aligned} \langle \mathbf{k}_2 \lambda_2 | \hat{\rho}_{\gamma_2} | \mathbf{k}_2 \lambda_2' \rangle &= \frac{1}{2j_i + 1} \frac{\varkappa}{2\pi} \sum_{\lambda_1 \lambda_1'} \sum_{m_i m_f} \sum_{M_1 M_1'} i^{M_1' - M_1} e^{i(M_1' - M_1)\phi_b} \\ &\times T_{m_f m_i}^{\lambda_2 \lambda_1}(M_1) T_{m_f m_i}^{\lambda_2' \lambda_1'}(M_1') J_{m - M_1}(\varkappa b) J_{m - M_1'}(\varkappa b) \langle \mathbf{k}_1 \lambda_1 | \hat{\rho}_{\gamma_1} | \mathbf{k}_1 \lambda_1' \rangle. \end{aligned} \quad (12)$$

Let us analyze the special case of atoms placed right on the beam axis ($b = 0$). In this scenario, the Bessel function from Eq. (12) is just $J_{m - M_1}(0) = \delta_{m M_1}$, so that the photon density matrix reads

$$\langle \mathbf{k}_2 \lambda_2 | \hat{\rho}_{\gamma_2} | \mathbf{k}_2 \lambda_2' \rangle = \frac{1}{2j_i + 1} \frac{\varkappa}{2\pi} \sum_{\lambda_1 \lambda_1'} \sum_{m_i m_f} T_{m_f m_i}^{\lambda_2 \lambda_1}(M_1 = m) T_{m_f m_i}^{\lambda_2' \lambda_1'}(M_1' = m) \langle \mathbf{k}_1 \lambda_1 | \hat{\rho}_{\gamma_1} | \mathbf{k}_1 \lambda_1' \rangle. \quad (13)$$

This expression indicates that the atom on the beam axis can just absorb a photon with the projection of the angular momentum m [29, 31]. In practice, however, it is difficult to position the atom just *on* the beam axis ($b = 0$). Therefore, in the next section we will consider the scattering of twisted light by a mesoscopic atomic target in which atoms are localized with nanometer precision.

D. Scattering on a mesoscopic atomic target

The experiments on the interaction of twisted light beams with the atoms or ions, which are localized in a small volume of several tens of nanometers by means of a microstructured Paul trap, are feasible today [29]. For the Rayleigh scattering by such a mesoscopic atomic target centered on the beam axis, the density matrix of scattered photons is given by [31, 35]

$$\begin{aligned} \langle \mathbf{k}_2 \lambda_2 | \hat{\rho}_{\gamma_2} | \mathbf{k}_2 \lambda_2' \rangle &= \frac{1}{2j_i + 1} \sum_{\lambda_1 \lambda_1'} \sum_{m_i m_f} \langle \mathbf{k}_1 \lambda_1 | \hat{\rho}_{\gamma_1} | \mathbf{k}_1 \lambda_1' \rangle \\ &\times \int f(\mathbf{b}) \mathcal{M}_{m_f m_i}^{\lambda_2 \lambda_1}(\mathbf{b}) \mathcal{M}_{m_f m_i}^{\lambda_2' \lambda_1'}(\mathbf{b}) d^2 \mathbf{b}, \end{aligned} \quad (14)$$

where the atomic density of this target in the transverse plane (cf. Fig. 1) is assumed to follow the Gaussian distribution [44]

$$f(\mathbf{b}) = \frac{1}{2\pi\sigma^2} e^{-\frac{b^2}{2\sigma^2}}. \quad (15)$$

In this formula, σ is the width of the target. After making use of the transition amplitude (10) and integrating over

the azimuthal angle ϕ_b , the photon density matrix for the mesoscopic atomic target becomes

$$\begin{aligned} \langle \mathbf{k}_2 \lambda_2 | \hat{\rho}_{\gamma_2} | \mathbf{k}_2 \lambda_2' \rangle &= \frac{1}{2j_i + 1} \frac{\varkappa}{2\pi\sigma^2} \\ &\times \sum_{\lambda_1 \lambda_1'} \sum_{m_i m_f M_1} \langle \mathbf{k}_1 \lambda_1 | \hat{\rho}_{\gamma_1} | \mathbf{k}_1 \lambda_1' \rangle T_{m_f m_i}^{\lambda_2 \lambda_1}(M_1) \\ &\times T_{m_f m_i}^{\lambda_2' \lambda_1'}(M_1) \int_0^\infty J_{m - M_1}^2(\varkappa b) e^{-\frac{b^2}{2\sigma^2}} b db. \end{aligned} \quad (16)$$

Both the density matrices (13) and (16) show that the polarization of outgoing photons depends on the TAM projection m of an incident Bessel beam in the elastic scattering by a single atom or by a mesoscopic atomic target. However, there is no m dependence for a rather large macroscopic atomic target, as we shall see below.

E. Scattering on a macroscopic atomic target

We next analyze the scattering of Bessel beam by a macroscopic target in which atoms are distributed randomly over the whole extent of the incident beam. In the case of such a large target, the photon density matrix is

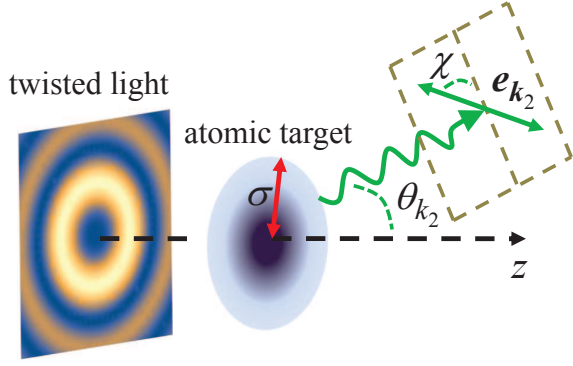


FIG. 1. Geometry of the Rayleigh scattering of twisted light by a mesoscopic atomic target of size σ . While the quantization (z) axis is taken along the propagation direction of the incident beam, the center of atomic target is placed on the beam axis. The emission direction of the outgoing photons is characterized by the angle θ_{k_2} , and their polarization vector \mathbf{e}_{k_2} is described by the angle χ .

defined by [28]

$$\begin{aligned}
\langle \mathbf{k}_2 \lambda_2 | \hat{\rho}_{\gamma_2} | \mathbf{k}_2 \lambda'_2 \rangle &= \frac{1}{2j_i + 1} \sum_{\lambda_1 \lambda'_1} \sum_{m_i m_f} \langle \mathbf{k}_1 \lambda_1 | \hat{\rho}_{\gamma_1} | \mathbf{k}_1 \lambda'_1 \rangle \\
&\times \int \mathcal{M}_{m_f m_i}^{\lambda_2 \lambda_1}(\mathbf{b}) \mathcal{M}_{m_f m_i}^{\lambda'_2 \lambda'_1 *}(\mathbf{b}) d^2 \mathbf{b} \\
&= \frac{1}{2j_i + 1} \sum_{\lambda_1 \lambda'_1} \sum_{m_i m_f} \sum_{M_1 M'_1} \langle \mathbf{k}_1 \lambda_1 | \hat{\rho}_{\gamma_1} | \mathbf{k}_1 \lambda'_1 \rangle \\
&\times \int a_{\mathcal{Z}m}(\mathbf{k}_{\perp 1}) a_{\mathcal{Z}m}^*(\mathbf{k}'_{\perp 1}) e^{-iM_1 \phi_{k_1} + iM'_1 \phi_{k'_1} + i(\mathbf{k}_{\perp 1} - \mathbf{k}'_{\perp 1}) \cdot \mathbf{b}} \\
&\times T_{m_f m_i}^{\lambda_2 \lambda_1}(M_1) T_{m_f m_i}^{\lambda'_2 \lambda'_1 *} (M'_1) \frac{d^2 \mathbf{k}_{\perp 1} d^2 \mathbf{k}'_{\perp 1} d^2 \mathbf{b}}{(2\pi)^4}, \quad (17)
\end{aligned}$$

As seen from these expressions, the Stokes parameters depend on the direction θ_{k_2} of scattered light. Therefore, in Sec. III we will use Eqs. (19) and (20) to investigate the polarization of outgoing photons for different scattering angles θ_{k_2} .

where we have used the transition amplitude (6). Here the integration over the impact parameter \mathbf{b} yields immediately the δ function $\delta(\mathbf{k}_{\perp 1} - \mathbf{k}'_{\perp 1})$. Moreover, if we perform the integration over the wave vector $\mathbf{k}'_{\perp 1}$ and over the azimuthal angle ϕ_{k_1} , we simply obtain $M_1 = M'_1$. We can further simplify the photon density matrix (17) by integrating over $k_{\perp 1}$, so that

$$\begin{aligned}
\langle \mathbf{k}_2 \lambda_2 | \hat{\rho}_{\gamma_2} | \mathbf{k}_2 \lambda'_2 \rangle &= \frac{1}{2j_i + 1} \sum_{\lambda_1 \lambda'_1} \sum_{m_i m_f M_1} T_{m_f m_i}^{\lambda_2 \lambda_1}(M_1) \\
&\times T_{m_f m_i}^{\lambda'_2 \lambda'_1 *} (M_1) \langle \mathbf{k}_1 \lambda_1 | \hat{\rho}_{\gamma_1} | \mathbf{k}_1 \lambda'_1 \rangle. \quad (18)
\end{aligned}$$

This formula shows that in the scattering on a macroscopic target the density matrix of outgoing photons and, hence, also their polarization are independent of the TAM projection m of incoming twisted light, but still depend on its helicity λ_1 and opening angle θ_{k_1} .

F. Polarization parameters

With the photon density matrices obtained above, we can now analyze the polarization of the Rayleigh scattered light. As usual in atomic and optical physics, the polarization properties of photons are characterized by the Stokes parameters [43]. In particular, the parameter $P_1 = (I_{\chi=0^\circ} - I_{\chi=90^\circ}) / (I_{\chi=0^\circ} + I_{\chi=90^\circ})$ characterizes the degree of linear polarization and is determined by the intensities I_χ of scattered light linearly polarized at an angle $\chi = 0^\circ$ or $\chi = 90^\circ$. Here the angle χ is defined with respect to the plane spanned by the directions of incident and outgoing photons (cf. Fig. 1). Another parameter P_2 , given by a similar ratio but for $\chi = 45^\circ$ and $\chi = 135^\circ$, is close to zero and therefore is not of interest. On the other hand, the nonzero parameter $P_3 = (I_{\lambda_2=+1} - I_{\lambda_2=-1}) / (I_{\lambda_2=+1} + I_{\lambda_2=-1})$ characterizes the degree of circular polarization and is determined by the intensities I_{λ_2} of outgoing circularly polarized photons with the helicity $\lambda_2 = \pm 1$. Both these Stokes parameters can be expressed in terms of the density matrix of photons as [43]

$$P_1(\theta_{k_2}) = -\frac{\langle \mathbf{k}_2 \lambda_2 = +1 | \hat{\rho}_{\gamma_2} | \mathbf{k}_2 \lambda'_2 = -1 \rangle + \langle \mathbf{k}_2 \lambda_2 = -1 | \hat{\rho}_{\gamma_2} | \mathbf{k}_2 \lambda'_2 = +1 \rangle}{\langle \mathbf{k}_2 \lambda_2 = +1 | \hat{\rho}_{\gamma_2} | \mathbf{k}_2 \lambda'_2 = +1 \rangle + \langle \mathbf{k}_2 \lambda_2 = -1 | \hat{\rho}_{\gamma_2} | \mathbf{k}_2 \lambda'_2 = -1 \rangle}, \quad (19)$$

$$P_3(\theta_{k_2}) = \frac{\langle \mathbf{k}_2 \lambda_2 = +1 | \hat{\rho}_{\gamma_2} | \mathbf{k}_2 \lambda'_2 = +1 \rangle - \langle \mathbf{k}_2 \lambda_2 = -1 | \hat{\rho}_{\gamma_2} | \mathbf{k}_2 \lambda'_2 = -1 \rangle}{\langle \mathbf{k}_2 \lambda_2 = +1 | \hat{\rho}_{\gamma_2} | \mathbf{k}_2 \lambda'_2 = +1 \rangle + \langle \mathbf{k}_2 \lambda_2 = -1 | \hat{\rho}_{\gamma_2} | \mathbf{k}_2 \lambda'_2 = -1 \rangle}. \quad (20)$$

G. Computations

Before we present our results for the Stokes parameters, let us briefly discuss some computational details. The evaluation of the polarization of scattered photons requires the knowledge of the reduced second-order tran-

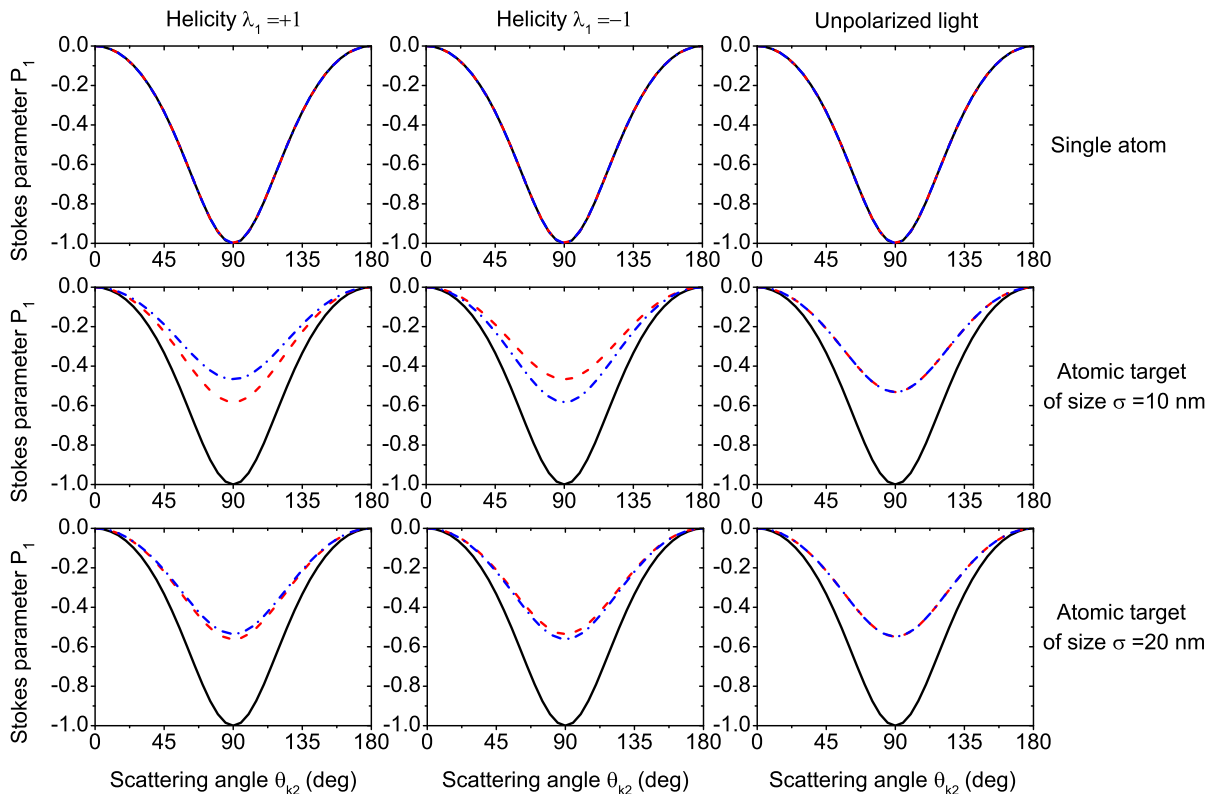


FIG. 2. Stokes parameters P_1 of Rayleigh scattered light on hydrogenlike C^{5+} ions in their ground state as a function of the emission angle θ_{k_2} . Results for incident plane waves (black solid lines) are compared with those for Bessel beams with TAM $m = +1$ (red dashed lines) and $m = -1$ (blue dash-dotted lines), respectively. Relativistic calculations were performed for a single atom (top row) and for mesoscopic atomic targets of size $\sigma = 10$ nm (middle row) and $\sigma = 20$ nm (bottom row), which are centered on the beam axis. Results are shown for different helicities λ_1 of the incident light: $\lambda_1 = +1$ (left column), $\lambda_1 = -1$ (central column), and for the unpolarized light (right column). Both the opening angle $\theta_{k_1} = 30^\circ$ of Bessel beams and the photon energy $\hbar\omega = 100$ eV are kept fixed.

sition amplitude (8), which involves the summation over the complete basis of the intermediate states $|n_\nu j_\nu\rangle$. In order to perform this summation, we use two independent approaches: the finite basis-set method and the Dirac-Coulomb Green's function (see Ref. [16] for further details). These two numerical methods provide identical results, which demonstrates the high accuracy of our calculations.

III. RESULTS AND DISCUSSION

In the previous sections we found the Stokes parameters P_1 and P_3 describing the polarization of scattered photons in the Rayleigh scattering of twisted Bessel beams by hydrogenlike ions. Such polarization parameters can be observed in current experiments [17] and are expressed in terms of the photon density matrix, as seen from Eqs. (19) and (20). We further analyze how these Stokes parameters of scattered light depend on its emission angle θ_{k_2} for incident Bessel beams with different projections m of the TAM, helicities λ_1 , and opening angles θ_{k_1} . In addition, we compare these parameters P_1

and P_3 for twisted light with those obtained for a plane-wave radiation of the same helicity incident along the z axis. Calculations were performed for the photon energy $\hbar\omega = 100$ eV and for three different targets of C^{5+} ions: a single atom (13), a mesoscopic target (16), and a macroscopic target (18) that are centered on the beam axis.

A. Polarization for a single atom and mesoscopic atomic target

We start with the first Stokes parameter P_1 that characterizes the degree of linear polarization of outgoing photons. Fig. 2 illustrates the parameter P_1 as a function of the emission angle θ_{k_2} for the Rayleigh scattering on a single atom (top row) as well as on the mesoscopic targets of size $\sigma = 10$ nm (middle row) and $\sigma = 20$ nm (bottom row). As seen from this figure, the outgoing photons are completely $P_1 = -1$ linearly polarized in the $\chi = 90^\circ$ direction at the scattering angle $\theta_{k_2} = 90^\circ$ for incoming plane waves (black solid lines). This is also true if a Bessel beam collides with a single atom located on

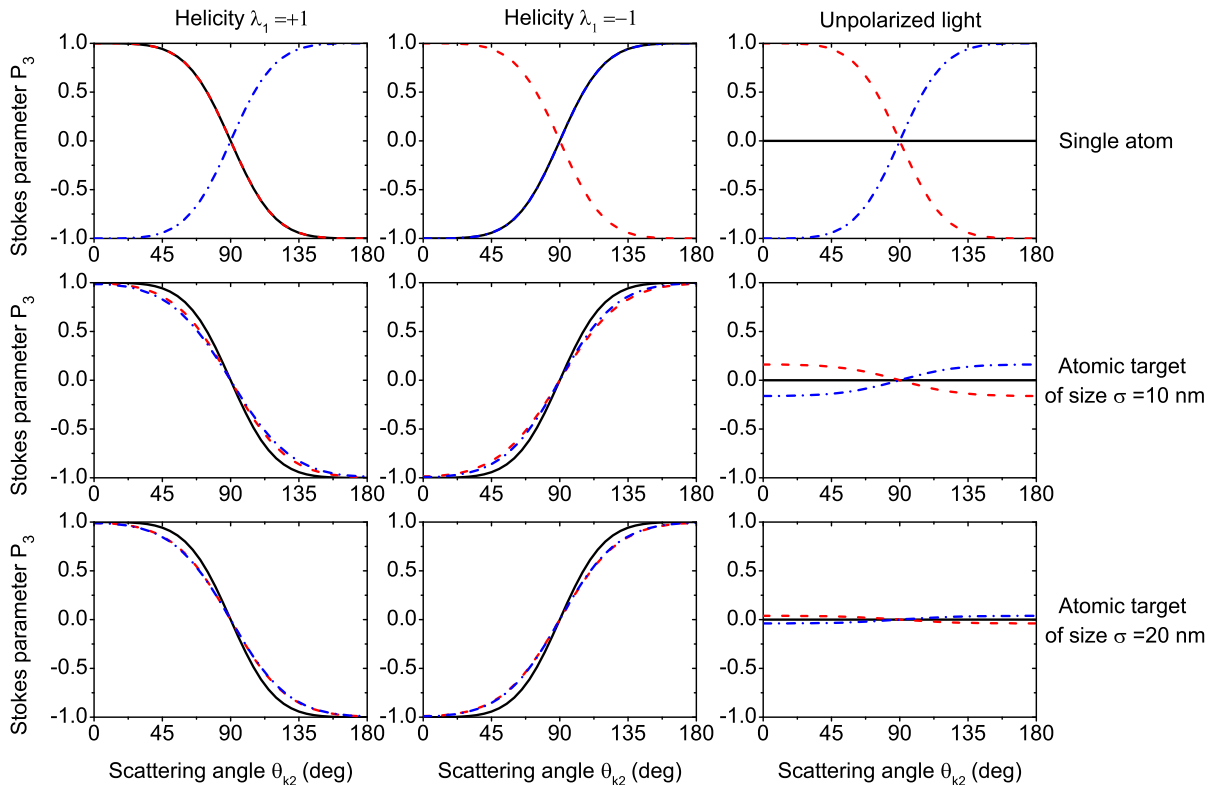


FIG. 3. Same as Fig. 2, but for the Stokes parameters P_3 of elastically scattered photons.

the beam axis. However, the scattering of such a Bessel beam by mesoscopic target with width $\sigma = 10$ nm, for example, leads to a significant decrease of the polarization at the angle $\theta_{k_2} = 90^\circ$, namely $P_1 = -0.58$ when $m = +1$ (red dashed line) or $P_1 = -0.47$ when $m = -1$ (blue dash-dotted line) for positive helicity $\lambda_1 = +1$, and vice versa for negative helicity $\lambda_1 = -1$. Thus the Stokes parameter P_1 of scattered photons depends on the TAM projection m of twisted light of a well-defined helicity λ_1 in the scattering by a mesoscopic target. On the other hand, P_1 is independent of TAM m if an incoming Bessel beam is unpolarized (cf. Fig. 2).

Up to this point, we have discussed the linear polarization of elastically scattered light. In order to analyze its degree of circular polarization, the third Stokes parameter P_3 as a function of the scattering angle θ_{k_2} is presented in Fig. 3. One sees that when the incident radiation is a plane wave of helicity λ_1 , the photons scattered in the forward ($\theta_{k_2} = 0^\circ$) direction are completely circularly polarized, namely $P_3 = 1$ if $\lambda_1 = 1$ or $P_3 = -1$ if $\lambda_1 = -1$. Moreover, the Stokes parameter P_3 of outgoing photons for the scattering of a twisted beam by a single atom on the beam axis coincides with the plane-wave results at all emission angles θ_{k_2} if the TAM projection of the beam is $m = \lambda_1$, as shown in Fig. 3. However, P_3 corresponding to twisted light shows the opposite behaviour to P_3 for the plane waves if the TAM projection is $m = -\lambda_1$. Such a difference in the polarization (or

helicity) of outgoing photons is caused by the conservation of the angular momentum projection: the helicity λ_2 of a photon emitted in the forward ($\theta_{k_2} = 0^\circ$) direction should be equal to the projection M_1 of the angular momentum of a photon absorbed by the atom on the beam axis, which is $M_1 = m$ for a Bessel beam (13), in contrast to $M_1 = \lambda_1$ for a plane wave.

Let us consider how the mesoscopic atomic target may affect the third Stokes parameter of scattered light. Eq. (16) implies that all possible projections M_1 of the angular momentum of incoming photons are able to contribute to the scattering of twisted light by mesoscopic target, in contrast to $M_1 = m$ for the scattering by a single atom. As a result, in the case of a mesoscopic target the parameter P_3 of outgoing photons for an incident Bessel beam is slightly different from that for a plane wave in the angular range $30^\circ \lesssim \theta_{k_2} \lesssim 70^\circ$ and $110^\circ \lesssim \theta_{k_2} \lesssim 150^\circ$, as can be seen from the middle and bottom rows of Fig. 3. In addition, the Stokes parameters P_1 and P_3 are quite different for the two TAM projections $m = \pm 1$ of the beam when the mesoscopic target is rather small ($\sigma = 10$ nm). However, Figs. 2 and 3 also show that this difference between the Stokes parameters for various TAM m decreases with increasing size of the target ($\sigma = 20$ nm).

Strong effects of “twistedness” in the polarization of scattered light can be observed also for an incoming unpolarized Bessel beam containing photons of both helicities $\lambda_1 = \pm 1$ but with a fixed TAM projection m . In

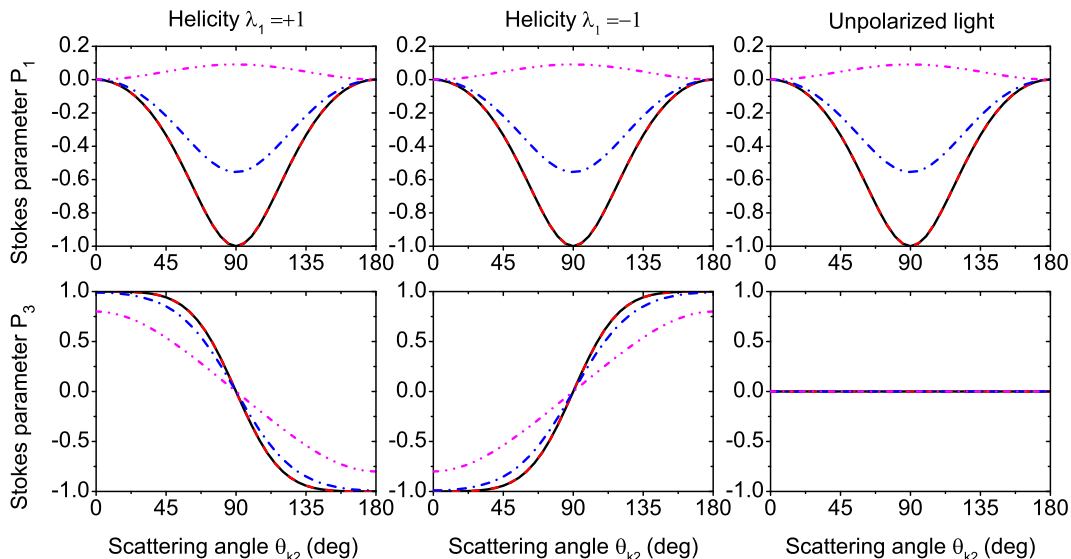


FIG. 4. Stokes parameters P_1 (top row) and P_3 (bottom row) of elastically scattered photons on hydrogenlike C^{5+} ions in their ground state for a macroscopic target. Plane-wave results (black solid lines) are compared with those for Bessel beams with opening angles $\theta_{k_1} = 1^\circ$ (red dashed lines), $\theta_{k_1} = 30^\circ$ (blue dash-dotted lines), and $\theta_{k_1} = 60^\circ$ (magenta dash-dot-dotted lines). Calculations were performed for different helicities λ_1 of the incident light: $\lambda_1 = +1$ (left column), $\lambda_1 = -1$ (central column), and for the unpolarized light (right column), when the photon energy $\hbar\omega = 100$ eV is fixed.

particular, Fig. 3 demonstrates that the Stokes parameter P_3 of outgoing photons is not always zero in the scattering of such a beam, in contrast to P_3 for incident unpolarized plane waves. For example, when the unpolarized twisted light with TAM projection $m = +1$ collides with a single atom, the third Stokes parameter (red dashed line) behaves similarly to that obtained for the incident beam with a well-defined helicity $\lambda_1 = +1$. This is because in the scattering of twisted light by a single atom P_3 does not depend on the helicity λ_1 , but is only sensitive to the TAM m . With increasing target size σ , however, the parameter P_3 for the case of unpolarized Bessel beam decreases and tends to zero as expected for incoming unpolarized plane waves (cf. Fig. 3).

B. Polarization for a macroscopic atomic target

Finally, we consider the scattering of twisted light by a macroscopic target as it occurs, for instance, for the scattering at a foil [17]. For such an extended target, the polarization of outgoing photons is independent of the TAM projection m of the twisted light, and as pointed out already in Sec. II E. In Fig. 4 we compare the two Stokes parameters P_1 and P_3 of the scattered light for different opening angles θ_{k_1} of Bessel beams with those for plane waves incident along the z axis. Similar as before, results were obtained as a function of the scattering angle θ_{k_2} for different helicities of the radiation. Here one can see that the parameters P_1 and P_3 for the scattering of a Bessel beam with a very small opening angle ($\theta_{k_1} = 1^\circ$) are almost identical to those as obtained for

an incident plane waves. However, the Stokes parameter P_1 behaves very differently for large opening angles ($\theta_{k_1} = 60^\circ$) and may become even positive at the emission angle $\theta_{k_2} = 90^\circ$. Moreover, for large angles θ_{k_1} , the circular polarization of the scattered photons is decreased in forward direction, for example $P_3 = \pm 0.8$ if the helicity of a Bessel beam is $\lambda_1 = \pm 1$. These modifications of the polarization of scattered light follow from Eq. (18) and imply that the scattering of a Bessel beam by macroscopic target can be considered as a scattering of plane waves propagating at the opening angle θ_{k_1} with respect to the quantization z axis.

IV. SUMMARY AND OUTLOOK

In summary, we explore the Rayleigh scattering of twisted light by hydrogenlike ions within the framework of second-order perturbation theory and Dirac's relativistic equation. In this analysis, we focused on the polarization of photons scattered by a single atom, by a mesoscopic target (atoms in a trap), or by a macroscopic target (foil). The polarization Stokes parameters of outgoing photons were calculated especially for hydrogenlike carbon and for incident twisted Bessel beams. We have shown that the linear and circular polarization of scattered light depends generally on the helicity λ_1 and the opening angle θ_{k_1} of Bessel beams, leading to Stokes parameters that differs quite significantly from the scattering of incident plane-wave photons. Moreover, the polarization of the scattered photons is very sensitive to the TAM projection m of twisted light for mesoscopic atomic

targets of a few tens of nm in size, while it remains unaffected by the TAM m in the case of a larger macroscopic target. Although our study was restricted to the scattering by hydrogenlike ions in their ground $1s$ state, similar polarization properties can also be observed in the scattering of twisted light by electrons in other s -shells. For example, we expect the same scattering polarization pattern for Ca^+ ions that were used in a recent experiment on the photoexcitation by twisted light [29]. Thus the Rayleigh scattering may serve as an accurate technique for measuring the properties of twisted beams in a wide range of photon energies, and in particular at rather high energies.

The interaction of twisted light with atoms may lead not only to the scattering of photons, but also to the

change in the atomic polarizability. The knowledge of the atomic polarizability induced by twisted radiation is very important in laser cooling and trapping experiments, and its analysis will be presented in a forthcoming publication.

ACKNOWLEDGMENTS

This work was supported by the DFG priority programme “Quantum Dynamics in Tailored Intense Fields”. A.A.P. acknowledges support from the Helmholtz Institute Jena and the Research School of Advanced Photon Science of Germany.

-
- [1] D. Brini, E. Fuschini, D. S. R. Murty, and P. Veronesi, *Nuovo Cimento* **11**, 533 (1959).
 - [2] S. C. Roy, B. Sarkar, L. D. Kissel, and R. H. Pratt, *Phys. Rev. A* **34**, 1178 (1986).
 - [3] F. Smend, D. Schaupp, H. Czerwinski, M. Schumacher, A. H. Millhouse, and L. Kissel, *Phys. Rev. A* **36**, 5189 (1987).
 - [4] P. P. Kane, L. Kissel, R. H. Pratt, and S. C. Roy, *Phys. Rep.* **140**, 75 (1986).
 - [5] M. Y. Sfeir, F. Wang, L. Huang, C.-C. Chuang, J. Hone, S. P. O’Brien, T. F. Heinz, and L. E. Brus, *Science* **306**, 1540 (2004).
 - [6] W. M. Elshemey, A. A. Elsayed, and A. El-Lakkani, *Phys. Med. Biol.* **44**, 2907 (1999).
 - [7] K. Maeda, Y. Terada, D. Kasen, F. K. Röpke, A. Bamba, R. Diehl, K. Nomoto, M. Kromer, I. R. Seitenzahl, H. Yamaguchi, T. Tamagawa, and W. Hillebrandt, *Astrophys. J.* **760**, 54 (2012).
 - [8] D. R. S. Somayajulu and V. Lakshminarayana, *J. Phys. A* **1**, 228 (1968).
 - [9] W. Chitwattanagorn, R. B. Taylor, P. Teansompramong, and I. B. Whittingham, *J. Phys. G* **6**, 1147 (1980).
 - [10] L. Kissel, R. H. Pratt, and S. C. Roy, *Phys. Rev. A* **22**, 1970 (1980).
 - [11] N. L. Manakov, A. V. Meremianin, A. Maquet, and J. P. J. Carney, *J. Phys. B* **33**, 4425 (2000).
 - [12] L. Safari, P. Amaro, S. Fritzsche, J. P. Santos, S. Tashenov, and F. Fratini, *Phys. Rev. A* **86**, 043405 (2012).
 - [13] A. Surzhykov, V. A. Yerokhin, T. Jahrsetz, P. Amaro, Th. Stöhlker, and S. Fritzsche, *Phys. Rev. A* **88**, 062515 (2013).
 - [14] A. Surzhykov, V. A. Yerokhin, Th. Stöhlker, and S. Fritzsche, *J. Phys. B* **48**, 144015 (2015).
 - [15] C.-P. Lin, K.-T. Cheng, and W. R. Johnson, *Phys. Rev. A* **11**, 1946 (1975).
 - [16] A. V. Volotka, V. A. Yerokhin, A. Surzhykov, Th. Stöhlker, and S. Fritzsche, *Phys. Rev. A* **93**, 023418 (2016).
 - [17] K.-H. Blumenhagen, S. Fritzsche, T. Gassner, A. Gumberidze, R. Martin, N. Schell, D. Seipt, U. Spillmann, A. Surzhykov, S. Trotsenko, G. Weber, V. A. Yerokhin, and T. Stöhlker, *New J. Phys.* **18**, 103034 (2016).
 - [18] J. Harris, V. Grillo, E. Mafakheri, G. Carlo Gazzadi, S. Frabboni, R. W. Boyd, and E. Karimi, *Nat. Phys.* **11**, 629 (2015).
 - [19] K. Y. Bliokh and F. Nori, *Phys. Rep.* **592**, 1 (2015).
 - [20] *The Angular Momentum of Light*, edited by D. L. Andrews and M. Babiker (Cambridge University Press, Cambridge, UK, 2013).
 - [21] M. Walde, A. Jost, K. Wicker, and R. Heintzmann, *Opt. Commun.* **383**, 64 (2017).
 - [22] K. Dota, A. Pathak, J. A. Dharmadhikari, D. Mathur, and A. K. Dharmadhikari, *Phys. Rev. A* **86**, 023808 (2012).
 - [23] O. Brzobohatý, T. Čížmár, and P. Zemánek, *Opt. Express* **16**, 12688 (2008).
 - [24] Yu. Yu. Choporova, B. A. Knyazev, G. N. Kulipanov, V. S. Pavelyev, M. A. Scheglov, N. A. Vinokurov, B. O. Volodkin, and V. N. Zhabin, *Phys. Rev. A* **96**, 023846 (2017).
 - [25] U. D. Jentschura and V. G. Serbo, *Phys. Rev. Lett.* **106**, 013001 (2011).
 - [26] S. Stock, A. Surzhykov, S. Fritzsche, and D. Seipt, *Phys. Rev. A* **92**, 013401 (2015).
 - [27] J. A. Sherwin, *Phys. Rev. A* **95**, 052101 (2017).
 - [28] A. Surzhykov, D. Seipt, V. G. Serbo, and S. Fritzsche, *Phys. Rev. A* **91**, 013403 (2015).
 - [29] C. T. Schmiegelow, J. Schulz, H. Kaufmann, T. Ruster, U. G. Poschinger, and F. Schmidt-Kaler, *Nat. Commun.* **7**, 12998 (2016).
 - [30] A. Afanasev, C. E. Carlson, and A. Mukherjee, *Phys. Rev. A* **88**, 033841 (2013).
 - [31] A. A. Peshkov, V. G. Serbo, S. Fritzsche, and A. Surzhykov, *Phys. Scr.* **91**, 064001 (2016).
 - [32] G. F. Quinteiro, D. E. Reiter, and T. Kuhn, *Phys. Rev. A* **95**, 012106 (2017).
 - [33] A. A. Peshkov, D. Seipt, A. Surzhykov, and S. Fritzsche, *Phys. Rev. A* **96**, 023407 (2017).
 - [34] O. Matula, A. G. Hayrapetyan, V. G. Serbo, A. Surzhykov, and S. Fritzsche, *J. Phys. B* **46**, 205002 (2013).
 - [35] A. Surzhykov, D. Seipt, and S. Fritzsche, *Phys. Rev. A* **94**, 033420 (2016).
 - [36] G. F. Quinteiro and J. Berakdar, *Opt. Express* **17**, 20465 (2009).

- [37] K. Köksal and F. Koç, *Comput. Theoret. Chem.* **1099**, 203 (2017).
- [38] N. Radwell, T. W. Clark, B. Piccirillo, S. M. Barnett, and S. Franke-Arnold, *Phys. Rev. Lett.* **114**, 123603 (2015).
- [39] A. M. Akulshin, R. J. McLean, E. E. Mikhailov, and I. Novikova, *Opt. Lett.* **40**, 1109 (2015).
- [40] A. I. Akhiezer and V. B. Berestetskii, *Quantum Electrodynamics* (Wiley, New York, 1965).
- [41] M. E. Rose, *Elementary Theory of Angular Momentum* (John Wiley & Sons, New York, 1957).
- [42] D. A. Varshalovich, A. N. Moskalev, and V. K. Khersonskii, *Quantum Theory of Angular Momentum* (World Scientific, Singapore, 1988).
- [43] V. V. Balashov, A. N. Grum-Grzhimailo, and N. M. Kabachnik, *Polarization and Correlation Phenomena in Atomic Collisions* (Springer-Verlag, Berlin, 2000).
- [44] J. Eschner, *Eur. Phys. J. D* **22**, 341 (2003).